Astron. Astrophys. 335, 207–217 (1998)

ASTRONOMY AND ASTROPHYSICS

The neutrino-induced neutron source in helium shell and r-process nucleosynthesis

D.K. Nadyozhin[1], **I.V. Panov**[1,2], **and S.I. Blinnikov**[1]

[1] Institute for Theoretical and Experimental Physics, B. Cheremushkinskaya St. 25, 117259 Moscow, Russia
[2] Max-Planck-Institut für Astrophysik, Karl-Schwarzschild-Strasse 1, Postfach 1523, D-85740 Garching, Germany

Received 5 March 1997 / Accepted 10 February 1998

Abstract. The huge neutrino pulse that occurs during the collapse of a massive stellar core, is expected to contribute to the origination of a number of isotopes both of light chemical elements and heavy ones. In particular, evaporation of neutrons from helium nuclei excited by neutrino-nuclear inelastic collisions, may result in the r-process as it was first discussed by Epstein et al. (1988). Here we consider mainly the possibility to obtain the considerable amount of neutrons owing to the neutrino breakup of helium nuclei. It is shown that, in general, the heating of stellar matter due to the neutrino scattering off electrons and the heat released from the neutrino-helium breakup followed by the thermonuclear reactions should be taken into account. On the base of kinetic network, using all the important reactions up to $Z = 8$, the main features and the time-dependent character of the neutrino-driven neutron flux are investigated.

The time-dependent densities of free neutrons produced in helium breakup, $Y_{\rm n}(t)$, were used to calculate the r-process nucleosynthesis with another full kinetic network for ~ 3200 nuclides. It was found that in the case of metal-deficient stars, $Z \lesssim 0.01\, Z_{\odot}$, the resulting density of free neutrons seems to be high enough to drive the r-process efficiently under favorable conditions. But it is impossible to obtain a sufficient amount of heavy nuclei in neutrino-induced r-process in a helium shell at radii $R > R_{\rm cr} \approx 10^9$cm. We speculate that to make the neutrino-induced r-process work efficiently in the shell, one has to invoke nonstandard presupernova models in which helium hopefully is closer to the collapsed core owing, for instance, to a large scale mixing or/and rotation and magnetic fields. Apart from this exotic possibility, the neutrino-induced nucleosynthesis in the helium shell is certainly not strong enough to explain the observed solar r-process abundances.

Key words: nuclear reactions – nucleosynthesis – abundances – supernovae: general

1. Introduction

About 20 years ago the gravitational collapse of massive stellar cores was recognized to be accompanied by a strong neutrino pulse, and a new branch of nucleosynthesis was born — the neutrino nucleosynthesis. The general scheme of the neutrino nucleosynthesis can be described briefly as follows (e.g., Nadyozhin, 1991). Electron neutrinos ν_e and antineutrinos $\tilde{\nu_e}$ can interact with different isotopes (A, Z) of chemical elements by means of both charged currents:

$$\nu_e + (A, Z) \rightarrow (A, Z+1)^* + e^- \,, \tag{1}$$

$$\tilde{\nu_e} + (A, Z) \rightarrow (A, Z-1)^* + e^+ \,, \tag{2}$$

and neutral ones:

$$\nu + (A, Z) \rightarrow (A, Z)^* + \nu' \,, \tag{3}$$

where $\nu = \nu_e, \tilde{\nu_e}, \nu_\mu, \tilde{\nu_\mu}, \nu_\tau$ and $\tilde{\nu_\tau}$. Since the typical muon and tau neutrino and antineutrino energies are sufficiently less than the rest mass of muon and tau-lepton, $\nu_\mu, \tilde{\nu_\mu}, \nu_\tau$ and $\tilde{\nu_\tau}$ interact only by means of neutral current. The resulting nuclei are generally produced in highly excited states indicated by asterisks. The states decay emitting basically neutrons, protons, and α-particles. The products of reactions (1)–(3) interact both with themselves and background nuclei to give rise to a number of issues of importance for the origin of chemical elements. The existence of the Gamow–Teller and Isobaric-Analog resonances is crucial for the efficiency of the neutrino nucleosynthesis (see Fuller & Meyer, 1995; Aufderheide et al., 1994; Panov, 1994, and references therein).

The beginning of this new issue of nucleosynthesis was marked by papers of Domogatsky & Nadyozhin (1977, 1978, 1980), Domogatsky & Imshennik (1982), and Domogatsky et al. (1978a,b) devoted to the neutrino-induced production of p-nuclei and a number of light isotopes such as ^{7}Li, ^{9}Be, and ^{11}B.

Epstein et al. (1988) (EHC hereafter) put forward an elegant idea that, under favorable conditions, the inelastic scattering of the muon and tau neutrinos off helium nuclei in the helium shell would be a good source of neutrons necessary to drive the r-process. They showed that the favorable conditions were low metallicity ($\sim 0.01\,{\rm Z}_{\odot}$) and not too large radius of the helium shell ($\sim 7\times10^8$ cm). Woosley et al. (1990) undertook a comprehensive study of the neutrino nucleosynthesis and demonstrated, in particular, that it was hard to reconcile EHC's statement with their supernova models (Woosley & Weaver, 1995) — the radius of the helium shell was large in their models and the burst

of nucleosynthesis stimulated by the shock wave, crossing over the helium shell in a few seconds after the collapse of a stellar core, was strong enough (according to their estimate) to reduce the importance of the previous work done by neutrinos. The astrophysical community gives credit to Weaver & Woosley for their presupernova models which are among the best nowadays. However, it would be premature to discard EHC's idea for the only reason that it does not fit these models. Although a major breakthrough in the understanding of the mechanism of Type II supernovae has been attained during last years, one cannot yet judge with full confidence such details of presupernova structure as the characteristics of chemical stratification just before and immediately after the onset of the neutrino pulse. The main uncertainties seem to be associated with the large scale properties of time-dependent convection (Bazan & Arnett, 1994) and with yet poorly studied effects of rotation at terminal stages of stellar evolution. It is plausible to imagine, for instance, the occurrence of aspherical hydrodynamic flows bringing helium closer to the stellar center than the radius of helium shell in spherically symmetric hydrostatic presupernova models.

Though a promising site for the r-process nucleosynthesis responsible for the solar r-process abundances is expected to be the neutrino-driven wind blowing for a few seconds from a newborn neutron star (Takahashi et al., 1994; Qian & Woosley, 1996; Hoffman et al., 1997), the possibility to create heavy elements in the helium shell still remains to be of interest. First of all this relates to a well developed r-process signature observed recently in the extremely metal poor stars (Cowan et al., 1996a, 1996b; Ryan et al., 1996; Sneden et al., 1996) and possibly to some special issues requiring the weak neutron fluxes such as the origin of some isotopic anomalies in meteorites (Clayton 1989).

The aim of our study in progress is to specify the conditions (in terms of helium shell radius, temperature, density, and metallicity) favorable for the neutrino-induced production of both light isotopes and free neutrons. Here preliminary results are reported on free neutron yields relevant to the r-process, which were already discussed briefly in Nadyozhin et al. (1996) and Nadyozhin & Panov (1997).

2. Properties of the neutrino flux and thermonuclear rates

We use the neutrino light curve calculated by Nadyozhin (1978) for the collapse of iron-oxygen star of $2M_\odot$ (Fig. 1). The total energy emitted by neutrinos and antineutrinos of all the flavors is equal to $\mathcal{E}_{\nu\tilde{\nu}} = 5.3\times10^{53}$ erg.

To obtain the neutrino luminosity in erg $s^{-1}$and total energy emitted by neutrinos at time t one has to multiply $l_\nu(t)$ and $E_\nu(t)$ by $\mathcal{E}_{\nu\tilde{\nu}}$. The neutrino light curve has a narrow maximum at $t = 0.023$ sec and a slowly decaying ($\tau \sim 22$ sec) long tail. The bulk of the available neutron star binding energy is radiated for as long time as ~ 20 sec rather than for 3 sec adopted by EHC and Woosley et al. (1990).

We assume that each neutrino flavor carries away the same energy equal to $\frac{1}{6}\,\mathcal{E}_{\nu\tilde{\nu}}$ and has the Fermi–Dirac thermal spectrum with zero chemical potential. The mean individual energies of

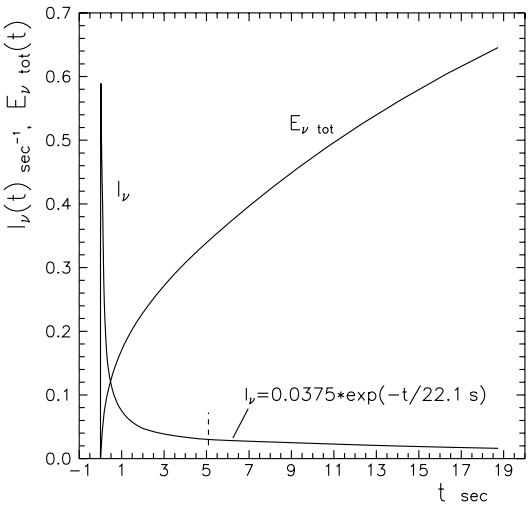

Fig. 1. The normalized neutrino light curve $l_\nu(t) = L_{\nu\tilde{\nu}}/\mathcal{E}_{\nu\tilde{\nu}}$ and integrated energy of the neutrino flux $E_{\nu tot}(t) = \int_0^t l_\nu\, dt$, $E_{\nu tot}(\infty) = 1$. ($\mathcal{E}_{\nu\tilde{\nu}}$ is the total energy emitted by neutrinos of all the flavors).

electron neutrinos and antineutrinos are taken to be equal to 12 MeV ($T_{\nu e} = 3.81$ MeV) whereas for muon and tau neutrinos and antineutrinos we have chosen a moderate value 25 MeV ($T_{\nu\mu\tau} = 7.94$ MeV). The cross section of excitation of ^{4}He by muon and tau neutrinos and the branching ratios for proton and neutron emission were calculated by EHC and Woosley et al. (1990) for the neutrino temperatures $T_{\nu\mu\tau} = 4 - 12$ MeV. We approximated their mean cross section (per helium nucleus and per neutrino flavor) by a simple equation

$$<\sigma_{\rm He4\nu}> = 5.28\times10^{-43}\, T^2_{\nu\mu\tau}\exp(-29.4/T_{\nu\mu\tau})\ {\rm cm}^2\,, \quad (4)$$

where $T_{\nu\mu\tau}$ is in MeV. Eq. (4) reflects the threshold nature of the process and has an accuracy better than 10% within all the temperature range involved (4–12 MeV).

The number of ^{4}He nuclei destroyed by neutrinos per unit time is given by

$$\dot{Y}_{\rm He4} = -B(t)\, Y_{\rm He4}\,; \quad B(t) \equiv q\,\frac{L_{\nu\tilde{\nu}}(t)<\sigma_{\rm He4\nu}>}{4\pi R^2 <E_\nu>} = \quad (5)$$
$$5.76\times10^{-2}\,\frac{l_\nu(t)}{R_8^2}\ {\rm s}^{-1}, \quad \left(R_8 = R/10^8{\rm cm}\right)\,,$$

where $q = 2/3$ is the fraction of muon and tau neutrinos and antineutrinos in the total neutrino flux; $L_{\nu\tilde{\nu}}$ is the total neutrino-antineutrino luminosity; R is the helium shell radius; and $<E_\nu>$ is the mean energy of muon and tau neutrinos and antineutrinos. The number of ^{4}He nuclei in unit volume $n_{\rm He4}$ is given by $n_{\rm He4} = \rho N_{\rm A} Y_{\rm He4}$, $N_{\rm A}$being Avogadro's number. So, $Y_{\rm He4}$ is the number of ^{4}He nuclei per baryon. The emission rates of neutrons and protons (and respectively of ^{3}He and ^{3}H) are

$$\dot{Y}_{\rm n} = \dot{Y}_{\rm He3} = -b_{\rm n}\dot{Y}_{\rm He4}\,, \qquad \dot{Y}_{\rm p} = \dot{Y}_{\rm H3} = -b_{\rm p}\dot{Y}_{\rm He4}\,, \quad (6)$$

where $b_{\rm n} = 0.471$ and $b_{\rm p} = 0.516$ are the branching ratios (Woosley et al., 1990).

To follow the sequence of thermonuclear reactions stimulated by the sources of fresh n, p, ^{3}He, and ^{3}H, we have used

Table 1. The list of nuclear reactions

^{1}H(n,γ)^{2}H + inv.	^{7}Li(α,γ)^{11}B	^{13}C(n,γ)^{14}C
^{2}H(p,γ)^{3}He + inv.	^{7}Li(α,n)^{10}B + inv.	^{13}C(α,n)^{16}O
^{2}H(p,n)2^{1}H	^{7}Be(p,γ)^{8}B + inv.	^{14}C(p,n)^{14}N
^{2}H(D,p)^{3}H	^{7}Be(D,p)2^{4}He	+ inv.
^{2}H(D,n)^{3}He	^{7}Be(T,np)2^{4}He	^{14}C(p,γ)^{15}N
^{3}H(p,γ)^{4}He	^{7}Be(^{3}He,2p)2^{4}He	^{13}N(p,γ)^{14}O
^{3}H(p,n)^{3}He + inv.	^{7}Be(α,γ)^{11}C	^{13}N(n,γ)^{14}N
^{3}H(D,n)^{4}He	^{7}Be(α,p)^{10}B + inv.	^{13}N(α,p)^{16}O
^{3}H(T,2n)^{4}He	^{9}Be(p,γ)^{10}B	^{14}N(p,γ)^{15}O
^{3}He(D,p)^{4}He	^{9}Be(p,np)2^{4}He [a]	^{14}N(α,γ)^{18}F
^{3}He(T,np)^{4}He	^{9}Be(p,D)2^{4}He	^{15}N(p,γ)^{16}O
^{3}He(T,D)^{4}He	^{9}Be(α,n)^{12}C [b]	^{15}N(p,α)^{12}C
^{3}He(^{3}He,2p)^{4}He	^{10}B(α,n)^{13}N	^{14}O(n,p)^{14}N
^{4}He(^{3}He,γ)^{7}Be + inv.	^{10}B(p,γ)^{11}C	^{15}O(n,p)^{15}N
^{4}He(T,γ)^{7}Li + inv.	^{11}B(p,γ)^{12}C	^{15}O(n,α)^{12}C
^{4}He(D,γ)^{6}Li + inv.	^{11}B(p,n)^{11}C + inv.	^{18}F(n,α)^{15}N
^{4}He(T,n)^{6}Li + inv.	^{11}B(α,p)^{14}C + inv.	"Fe"(n,γ)
^{4}He(^{3}He,p)^{6}Li + inv.	^{11}B(α,n)^{14}N + inv.	"Fe"(p,γ)
^{4}He(2α, γ)^{12}C	^{11}B(p,2α)^{4}He	
^{4}He(αn,γ)^{9}Be + inv.	^{11}C(p,γ)^{12}N + inv.	
^{6}Li(α,p)^{9}Be + inv.	^{11}C(n,γ)^{12}C	
^{6}Li(α,γ)^{10}B	^{11}C(n,2α)^{4}He	
^{6}Li(p,γ)^{7}Be	^{11}C(α,p)^{14}N + inv.	
^{7}Li(p,n)^{7}Be + inv.	^{12}C(p,γ)^{13}N + inv.	
^{7}Li(p,α)^{4}He	^{12}C(n,γ)^{13}C	
^{7}Li(D,n)2^{4}He	^{12}C(α, γ)^{16}O [c]	
^{7}Li(T,2n)2^{4}He	^{13}C(p,γ)^{14}N	
^{7}Li(^{3}He,np)2^{4}He	^{13}C(p,n)^{13}N + inv.	

[a] The reaction goes through unstable ^{9}B$\rightarrow$ 2^{4}He+p (life time $\sim 1\times10^{-16}$ s).
[b] The rate is taken from Wrean et al. (1994).
[c] The rate is multiplied by constant 1.7 (Weaver and Woosley, 1993).

Table 2. The weak interaction processes

^{4}He(ν, ν')^{4}He*	μ and τ neutrinos and antineutrinos,
^{4}He* $\rightarrow^{3}$H +p	the cross sections and branching ratios
^{4}He* $\rightarrow^{3}$He+n	from Woosley et al. (1990).
^{1}H($\tilde{\nu}_e$, e^{+})n	
^{8}B$\rightarrow$ 2 ^{4}He+e^{+}	$\tau = 0.770$ s
^{12}N$\rightarrow$ ^{12}C +e^{+}	$\tau = 0.011$ s
^{15}O$\rightarrow$ ^{15}N +e^{+}	$\tau = 122$ s
	The lifetimes τ from Tuli (1990)

a code connecting 26 nuclides from neutrons and protons up to ^{16}O with a net of about 100 most important direct and inverse reactions presented in Tables 1 and 2. The reaction rates were taken mostly from Caughlan & Fowler (1988) and from the updated version of Thielemann's original compilation (Thielemann et al., 1986).

The equations of nuclear kinetics were calculated both for constant values of density and temperature and for time-dependent temperature induced by the heating of stellar matter owing to the neutrino-helium interaction and neutrino-electron scattering.

3. Neutrino heating of stellar matter

There are two sources of heat worth to be accounted for in the helium shell. They are the neutrino scattering off electrons and the heat released during the neutrino-helium breakup and the subsequent thermonuclear reactions.

3.1. Neutrino-electron scattering

The differential cross section of the neutrino scattering off electrons at rest ($E_\nu \gg kT$), is given by (e.g., Okun, 1982; Vogel & Engel, 1989)

$$\frac{d\sigma}{d\varepsilon} = S_0 \left[(g_V + g_A)^2 + (g_V - g_A)^2 \left(1 - \frac{\varepsilon}{E_\nu}\right)^2 + \left(g_A^2 - g_V^2\right) \frac{\varepsilon}{E_\nu^2} \right], \quad (7)$$

where $S_0 = 2.20\times10^{-45}$ cm^2, E_ν and ε are the energy of incident neutrino and the recoil kinetic energy of electron, respectively (both in terms of $m_e c^2$), and

$$\begin{aligned} g_V &= \begin{cases} 2\sin^2\Theta_{\rm W} + \frac{1}{2} & \text{for } \nu_e, \\ 2\sin^2\Theta_{\rm W} - \frac{1}{2} & \text{for } \nu_\mu,\ \nu_\tau, \end{cases} \\ g_A &= \begin{cases} \frac{1}{2} & \text{for } \nu_e, \\ -\frac{1}{2} & \text{for } \nu_\mu,\ \nu_\tau. \end{cases} \end{aligned} \quad (8)$$

Here $\Theta_{\rm W}$ is the Weinberg angle ($\sin^2\Theta_{\rm W} = 0.23$). For antineutrinos, one must make the substitution $g_A \rightarrow -g_A$. The kinetic energy ε depends on the angle of scattered neutrino and varies within the limits

$$0 \le \varepsilon \le \varepsilon_m = \frac{2E_\nu^2}{1 + 2E_\nu}\,. \quad (9)$$

Integrating $\varepsilon d\sigma/d\varepsilon$ over the electron kinetic energy in the limits given by Eq.(9) and averaging over the Fermi–Dirac neutrino spectrum, we obtain

$$\left\langle \varepsilon \frac{d\sigma}{d\varepsilon} \right\rangle = S_0 \sum_i q_i \left(\frac{F_4(0)}{F_3(0)} \frac{kT_i}{m_e c^2}\, a_i - b_i \right), \quad (i = \nu_e, \tilde{\nu}_e, \nu_\mu, \tilde{\nu}_\mu, \nu_\tau, \tilde{\nu}_\tau)\,, \quad (10)$$

where

$$a_i = \frac{1}{12}\left(7g_V^2 + 7g_A^2 + 10 g_V g_A\right)_i\,,$$

$$b_i = \frac{1}{6}\left(5g_V^2 + g_A^2 + 6 g_V g_A\right)_i\,,$$

q_i and T_i are the fraction in the total neutrino luminosity and the Fermi–Dirac temperature of type i neutrinos, respectively; $F_4(0)$ and $F_3(0)$ are the Fermi–Dirac functions ($F_4(0)/F_3(0) = 4.106$). Deriving Eq.(10), we have neglected small terms of the order of $(m_e c^2/E_\nu)^2$.

The rate of energy release per unit mass, Q_s is given by

$$Q_s = \frac{1}{2}(1 + {\rm X}) N_{\rm A} \frac{L_{\nu\tilde{\nu}}}{4\pi R^2} \left\langle \varepsilon \frac{d\sigma}{d\varepsilon} \right\rangle\,. \quad (11)$$

Here X is the mass fraction of hydrogen (in the helium shell X= 0).

Assuming $q_i = 1/6$, we obtain numerically

$$Q_s \;=\; 1.267\times10^{16}\,\frac{l_\nu(t)}{R_8^2}\cdot$$

$$(0.4027\,T_{\nu e} + 0.1730\,T_{\nu\mu\tau} - 0.0657)\ \mathrm{erg\ g^{-1}s^{-1}}\,, \quad (12)$$

where $T_{\nu e}$ and $T_{\nu\mu\tau}$ are in MeV and $R_8 = R/10^8$cm. Since $T_{\nu\mu\tau} \approx 2T_{\nu e}$, the contribution of muon and tau neutrino and antineutrino scattering to heating is almost equal to that of the electron neutrino and antineutrino.

3.2. Neutrino-helium breakup and thermonuclear reactions

The neutrino-helium breakup supplies heat in the form of kinetic energy of the resulting fragments p, n, ^{3}H, and ^{3}He, which is equal to the difference between the excitation energy E^* and binding energy, $B_{\rm He4}$, of ^{4}He with respect to ^{3}H+p and ^{3}He+n. Thus, the total release of heat per reaction is $E^* - B_{\rm He4}$ with $B_{\rm He4} \approx 20.6$ MeV and ≈ 19.8 MeV for the proton and neutron channels, respectively. The general expression for the rate of energy release per unit mass due to the neutrino-helium breakup is given by

$$Q_B \;=\; N_{\rm A}\,Y_{\rm He4}\frac{L_{\nu\tilde\nu}}{4\pi R^2}\sum_i q_i\left[<\sigma_{\rm He4i}>\frac{(E^*-B_{\rm He4})_i}{<E_{\nu i}>}\right],$$

$$(i=\nu_e,\tilde\nu_e,\nu_\mu,\tilde\nu_\mu,\nu_\tau,\tilde\nu_\tau)\,, \quad (13)$$

where $(E^* - B_{\rm He4})_i$ is a branching-ratio averaged value and the Fermi–Dirac average energy of individual neutrinos $<E_{\nu i}> = 3.147kT_i$.

To estimate the rate of energy liberation in the thermonuclear reactions, one has to find a difference between the total binding energies of composition on two successive time steps of calculations, on line with the integration of the equations of nuclear kinetics. However, we shall use a simple approximation here. The point is that the thermonuclear reactions reassemble rapidly the bulk of the neutrino-destroyed helium and convert the rest of it into heavier nuclei (such as ^{7}Li, ^{11}B, ^{12}C and others), thereby returning the binding energy of ^{4}He back in the form of heat. To take this effect into account, it is sufficient to neglect the binding energy $B_{\rm He4}$ in Eq.(13). Such a procedure slightly underestimates the energy release since the energy liberated in processing of ^{4}He into heavier nuclei happens to be omitted. Assuming $B_{\rm He4} = 0$ in Eq.(13), neglecting the electron neutrinos and antineutrinos, specifying $Y_{\rm He} = 1/4$, $E^* = 36$MeV (Woosley et al., 1990), and $\sum q_i = 2/3$, and using Eq.(4) for $<\sigma_{\rm He4i}>$, we obtain numerically

$$Q_B \;=\; 2.557\times10^{18}\,\frac{l_\nu(t)}{R_8^2}\,T_{\nu\mu\tau}\exp(-29.4/T_{\nu\mu\tau}) \;=$$

$$5.017\times10^{17}\,\frac{l_\nu(t)}{R_8^2}\ \mathrm{erg\ g^{-1}s^{-1}}\,, \quad (14)$$

where we made also a substitution $T_{\nu\mu\tau} = 7.94$ MeV.

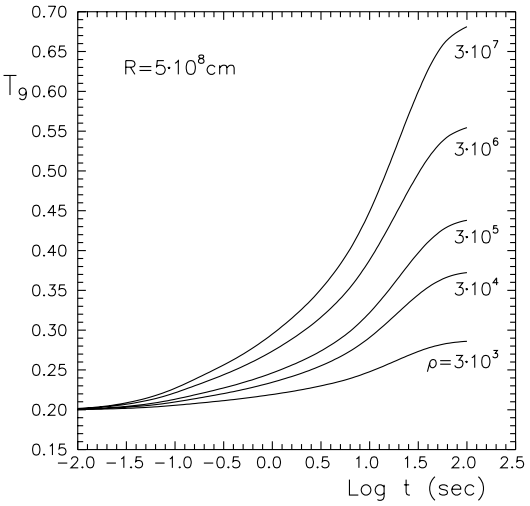

Fig. 2. Temperature versus time as a result of the neutrino heating. The initial temperature $T_9(0) = 0.2$.

3.3. Neutrino heating

For simplicity we assume that density ρ and radius R of the helium shell remain unchanged during the heating. This is certainly true for the initial narrow peak of the neutrino luminosity (Fig. 1). However, the time scale of the neutrino light curve tail is comparable to the hydrodynamic time scale in the helium shell, $\sim R/v_{\rm sound}$, and such an assumption slightly overestimates the resulting increase in temperature. To obtain the temporal behavior of temperature, one has to integrate over time the thermodynamic equation of energy:

$$E(T,\rho) \;=\; E(T_0,\rho) \;+\; \int_0^t (Q_S + Q_B)\,dt\,, \quad (15)$$

where E is specific energy. For E, we use the Equation of State as given by Blinnikov et al. (1996) which takes into account ideal electron-positron gas with an arbitrary degree of degeneration, ideal ion gas, and blackbody radiation.

Fig. 2 shows temperature as a function of time for different ρ as calculated with Eq.(15). For initial temperature $T_9 = 0.2$, density $\rho = 3\times10^3$ g cm^{-3}, and radius $R = 5\times10^8$ cm of the helium shell, the heating is noticeable but not crucial — T_9 increases up to ≈ 0.25 in 10 sec after the onset of the neutrino flux. The greater density, the stronger heating — for instance, at $\rho = 3\times10^5$ g cm^{-3}, temperature increases up to 0.32. Since the heating scales also as R^{-2}, it must be taken into account in the calculations of the neutrino nucleosynthesis at radii $R \lesssim 5\times10^8$ cm (especially for the carbon and silicon shells).

4. Neutrino-induced production of neutrons

A number of calculations were made for different (including extreme) assumptions of initial amounts of iron and ^{14}N and of the helium shell radius R, as well. The temporal behavior of neutron yield $Y_{\rm n}$ is shown in Fig. 3 for $R = 5\times10^8$ cm, $T_9 = 0.2$, $\rho = 3\times10^3$ g cm^{-3}, Z $= 0.01$Z$_\odot$, and different assumptions

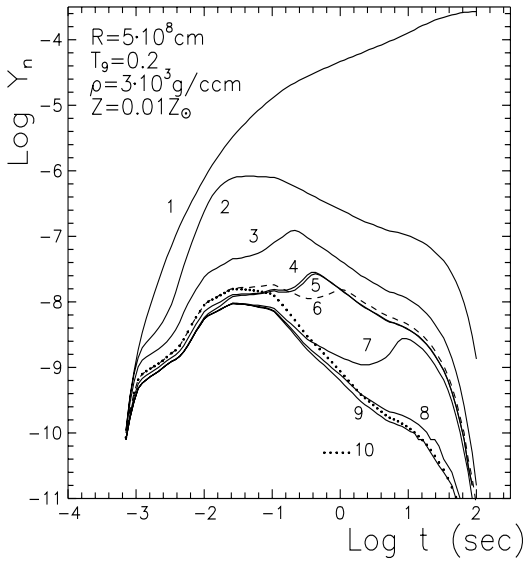

Fig. 3. The neutron abundance versus time.
The curves labelled by numbers correspond to the cases:

1 Neutron yield from the neutrino-helium inelastic scattering (all the nuclear reactions being turned off).
2 No "Fe" and no initial ^{14}N.
3 No ^{14}N, the burning rate of Fe is slowed by a factor of 30.
4 No Fe and the CNO fraction of initial ^{14}N.
5 Cosmic initial fraction of Fe and CNO fraction of ^{14}N; Fe burns via ^{56}Fe(n,γ) reaction.
6 A half of CNO fraction of ^{14}N, the burning rate of Fe is slowed by a factor of 30 (dashed curve).
7 Same as Case 6 but CNO fraction of ^{14}N.
8 The CNO fraction of ^{14}N and burning rate of Fe is slowed by a factor of 100.
9 Same as 5 but no burning of Fe ($Y_{\rm Fe}$=const).
10 Same as 6, but no burning of Fe (dotted curve).

about the neutron poisons ^{14}N and ^{56}Fe. The neutron density $n_{\rm n}(t) = \rho N_{\rm A} Y_{\rm n}(t) = 1.81\times10^{27}\, Y_{\rm n}(t)\,{\rm cm}^{-3}$.

Even with no initial ^{14}N and Fe (Case 2), the neutron density falls substantially (by about 4 orders of magnitude during the first 10 s) as compared to the amount supplied by the neutrino-helium inelastic scattering (Case 1) [1]. This happens because the bulk of the neutrino-destroyed ^{4}He proves to be reassembled mostly through ^{1}H(n,γ)^{2}H, ^{3}He(n,p)^{3}H, ^{2}H(D,p)^{3}H, ^{3}He(D,p)^{4}He, ^{3}H(D,n)^{4}He, ^{3}He(T,D)^{4}He, and ^{3}H(T,2n)^{4}He reactions. Only as little as $\sim$1% of the ^{4}He breakup products is left unbound back into ^{4}He to synthesize some ^{7}Li [mostly through the reaction ^{4}He(T,γ)^{7}Li] and other less abundant species such as ^{11}B, ^{13}C, and ^{14}C.

In Case 4, there is no Fe and the initial fraction of ^{14}N is equal to the cosmic fraction of CNO-isotopes multiplied by a factor of 0.95 as it follows from the hydrogen burning in well developed CNO-cycle ($Y_{\rm N14} = 0.95\,{\rm X_{CNO}}/14 = 0.0523{\rm Z}$). The same initial value of $Y_{\rm N14}$ was chosen also for Cases 5, 7, 8, and 9. For the versions described by Cases 5–9, the initial abundance of Fe was assumed to be equal to its cosmic value of $Y_{\rm Fe56} = {\rm X_{Fe}}/56 = 1.27\times10^{-3}\,{\rm Z}$ (Anders & Grevese, 1989). The difference between Cases 5 and 4 is that in Case 5 the initial abundance of Fe was taken equal to its cosmic value but Fe was burning at the rate

$$\frac{dY_{\rm Fe}}{dt} = -\rho N_{\rm A} < \sigma v >_{{\rm Fen}\gamma} Y_{\rm n} Y_{\rm Fe}\,. \qquad (16)$$

Since the number of the neutrino-produced neutrons (Case 1) exceeds considerably the initial number of Fe-nuclei, it takes only about 0.05 sec to burn out virtually all Fe. That is why one can hardly notice the difference between Cases 4 and 5. This is, of course, an unreal assumption. The products of Fe burning still continue to absorb neutrons. To simulate this effect we calculated two more versions with the rate of Fe-burning decreased by factors 30 and 100 (Cases 7 and 8, respectively). In other words, we have changed Eq.(16) by multiplying its right-hand side by an additional factor of 1/30 or 1/100. However, in the equation for $dY_{\rm n}/dt$, the rate of the neutron absorption by Fe remained unchanged and equal to the unmodified right-hand side of Eq.(16). This means that $Y_{\rm Fe}$ begin to decrease substantially after capturing 30 or 100 neutrons. The factor 1/30 in the right-hand side of Eq.(16) seems to be a good compromise to simulate the consumption of neutrons in the r-process. In Case 9, Fe does not burn at all. In Cases 4–6, the neutron abundance reaches the magnitude of $Y_{\rm n} \sim 10^{-8}$ and keeps it as long as about 5 sec. The duration of the plateau in Cases 7–8 is much shorter than for Cases 4–6. The comparison of Case 10 with Case 6 shows how strongly $Y_{\rm n}$ depends on the parameters of Fe-burning at $t \gtrsim 1$ sec.

The initial abundance of ^{14}N, equal to the total amount of CNO isotopes, is certainly the upper limit. In moderately massive stars (10–15M$_\odot$), the CNO-cycle is hardly to be efficient enough to convert all ^{16}O into ^{14}N. Thus, it is reasonable to take a lower initial abundance of ^{14}N. In Case 6, $Y_{\rm n}$ was calculated with $Y_{\rm N14\,initial} = 0.5{\rm X_{CNO\,cosmic}}/14$ (which gives $Y_{\rm N14}/Y_{\rm Fe} \approx 20$ — the value accepted by EHC) and the rate of Fe-burning decreased by a factor of 30. This set for properties of the neutron poisons ^{14}N and Fe will be considered as standard in our further preliminary r-process calculations.

The resulting $Y_{\rm n}$ proved to be strongly sensitive to the helium shell radius R (Fig. 4). For instance for $R = 10^9$cm, $Y_{\rm n}$ attains a maximum $Y_{\rm n\,max} \approx 10^{-9}$ which is about an order of magnitude less than for $R = 5\times10^8$ cm and lasts only for ~ 0.2 sec rather than ~ 5 sec as in Case 6.

The dependence of $Y_{\rm n}$ on temperature turns out to be more complicated (Fig. 5). The solid lines correspond to constant temperatures $T_9 = 0.2$ (Case 6), 0.3, 0.5, and 0.8 whereas the dashed one shows the effect of neutrino heating for initial temperature $T_9 = 0.2$ with $T_9(t)$ given by the lower curve in Fig. 2. The neutron yield falls abruptly even for a moderate increase in T. However at temperatures $T_9 \gtrsim 0.8$, it starts to grow at the very beginning of the neutrino flux ($t \lesssim 0.1$ sec). This happens

[1] According to Eqs. (5,6), the total amount of neutrons produced by the neutrino breakup of ^{4}He is equal to $Y_{\rm n} = 5.76\times10^{-2}\, b_{\rm n} Y_{\rm He4}/R_8^2 \approx 2.7\times10^{-4}$ for $R_8 = 5$.

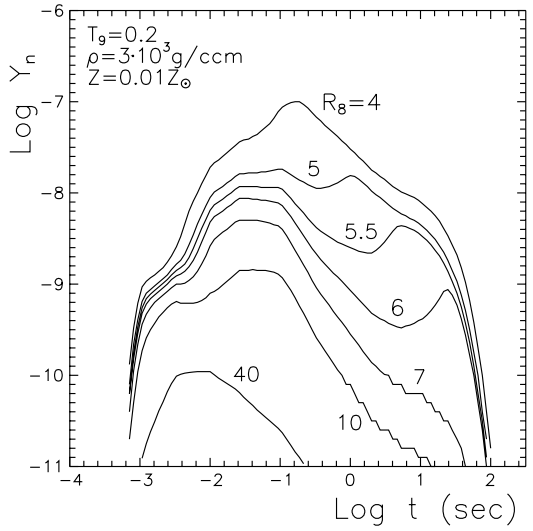

Fig. 4. Neutron abundance versus time for different radii of helium shell.

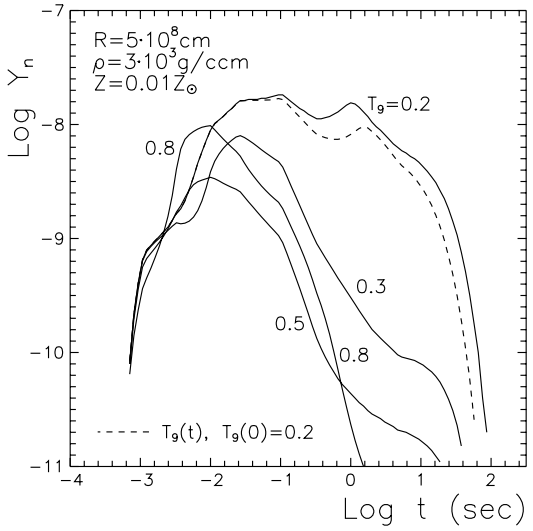

Fig. 5. Neutron abundance versus time for different temperatures of helium shell.

owing to a considerable rise in the rates of (p,n), (α,n), and (γ,n) reactions. The possibility of the neutrino-driven r-process at temperatures as high as $T_9 \sim 2$ seems to deserve further and more detailed investigation.

5. The r-process

The time-dependent neutron yield $Y_{\rm n}(t)$ discussed above can now be used to calculate the r-process. Instead of rough approximations for $Y_{\rm n}(t)$ imitating Case 6 in our previous calculations (Nadyozhin et al., 1996, Versions I and II), we used the time-dependent neutron yield exactly as shown for Case 6 in Fig. 3 and its analog for $R = 10^9$ cm (the curve $R_8 = 10$ in Fig. 4) to fulfill the r-process calculations. Such an approximate approach to connect the two codes, through the neutron abundance $Y_{\rm n}(t)$ seems to be adequate for our preliminary study. The accuracy of the approximation is briefly discussed in Appendix A.

The r-elements yields were estimated with the aid of the kinetic model of nucleosynthesis developed earlier by Blinnikov & Panov (1996). In this model, variations in the number density $n(A, Z)$ of each nuclide were determined taking into account reactions involving neutrons and β-decays :

$$
\begin{aligned}
dY_{A,Z}/dt = &-\lambda_{\gamma{\rm n}}(A,Z)\cdot Y_{A,Z} - \lambda_\beta(A,Z)\cdot Y_{A,Z} - \\
&Y_{\rm n}(t)\rho N_{\rm A} <\sigma_{{\rm n}\gamma}(A,Z)v> Y_{A,Z} + \\
&\lambda_{\gamma{\rm n}}(A+1,Z)\cdot Y_{A+1,Z} + \\
&Y_{\rm n}(t)\rho N_{\rm A} <\sigma_{{\rm n}\gamma}(A-1,Z)v> Y_{A-1,Z} + \\
&\lambda_{\nu e}(A,Z-1)\cdot Y_{A,Z-1} - \lambda_{\nu e}(A,Z)\cdot Y_{A,Z} + \\
&\sum_{i=0,1,2,3} \lambda_\beta(A+i,Z-1)\cdot P_i(A+i,Z-1) \\
&\cdot Y_{A+i,Z-1} \ , \qquad (17)
\end{aligned}
$$

$$
\begin{aligned}
dY_{\rm n}/dt = \sum_{A,Z}\Bigg[&\lambda_{\gamma{\rm n}}(A,Z) - Y_{\rm n}(t)\rho N_{\rm A} <\sigma_{{\rm n}\gamma}(A,Z)v> \\
&+ \sum_{i=1,2,3} i\cdot\lambda_\beta(A,Z)\cdot P_i(A,Z)\Bigg] Y_{A,Z} \ , \qquad (18)
\end{aligned}
$$

where

$$
Y_{A,Z} = \frac{n(A,Z)}{\rho N_{\rm A}} \ , \qquad Y_{\rm n}(t) = \frac{n_{\rm n}(t)}{\rho N_{\rm A}} \ . \qquad (19)
$$

In addition to equations given by Blinnikov & Panov (1996), Eqs. (17,18) contain terms describing the beta-delayed emission of neutrons, $P_i(A, Z)$ being the probability of emission of i neutrons, ($\sum_{i=0,1,2,3} P_i = 1$). However, in the present calculations we take into account the beta-delayed emission of only one neutron, namely we assume $P_2 = P_3 = 0$. Eq. (18) for $dY_{\rm n}/dt$ is not used here since $Y_{\rm n}(t)$ was taken from Case 6 in Fig. 3.

Moreover, we have also added terms accounting for the capture of *electron* neutrinos by nuclei with reaction rates $\lambda_{\nu e}(A, Z)$. The relative role of the ν_e-capture in Eq.(17) turns out to be insignificant for the environments under consideration. The contribution of the $\tilde{\nu}_e$-capture is even smaller owing to a high threshold for the neutron-rich nuclei, and we neglect it. The neutrino-nuclear cross sections were calculated earlier (Panov, 1994; cf. Fuller & Meyer, 1995; McLaughlin & Fuller, 1995), with both Isobar-Analog and Gamow–Teller resonances taken into account. The hope to obtain a noticeable smoothing of the abundance curve of the r-process elements due to the neutrino-nuclear interaction, seems hardly to be realized since the cross sections $\sigma_{\nu e}(A, Z)$ themselves demonstrate a clear even-odd effect that is decreasing, however, in magnitude when A and Z are increasing. The r-process calculations, fulfilled here with account for the capture of the *electron* neutrinos by nuclei, manifested only one noticeable effect — the acceleration of the r-process, as it was shown by Nadyozhin & Panov (1993). However, in case of a larger contribution of the neutrino-capture

reactions to the r-process or under the conditions of lower neutron fluxes involved (owing, for instance, to the exhaustion of neutrons at the very end of the r-process), neutrinos would be able to decrease the even-odd effect to some extent (Panov, in preparation). It should be mentioned that our calculations do not take into account the evaporation of nucleons from highly excited states of daughter nuclei. This effect seems to be only of minor importance for the bulk of stable nuclei synthesized in the r-process (Meyer et al., 1992) except for the production of p-nuclei (Domogatsky & Nadyozhin, 1977, 1978).

It is quite appropriate to notice here that the calculations of σ_ν for neutrinos from collapsed stellar cores in the approximation of the GT-resonance energy shape with the delta function (Fuller & Meyer, 1995; McLaughlin & Fuller, 1995), are accurate enough only when $< E_\nu > \approx E_{\rm GTR}$. However, in case of typically short-living nuclei along the r-process path, the GT-resonance energy proves to be rather high (Panov, 1994) and one has to deal with a detailed shape of GT-strength function in more accurate calculations.

The boundary conditions for the range of the nuclei involved into consideration, were specified in the following way: $Z_{\rm min}$=26 and $Z_{\rm max}$=95, with the minimum and maximum A for each Z being determined by the lightest stable nucleus from one side, and by the neutron-drip line for the heaviest isotope from the other side. Although we did not take into account the proton-rich unstable nuclei, the full number of nuclides and kinetic equations involved in our calculations was as large as about 3200 (the strict number depended on mass formulae used). The reaction rates entering Eqs. (17) differ by tens orders of magnitude. Thus, the system of equations for nuclear kinetics, to be dealt with, is a classical example of a stiff system of ordinary differential equations. In our calculations, we used one of the most effective methods to solve such a stiff system of equations — Gear's method (Gear, 1971). Our code has options permitting also to make use of the implicit Adams method and the method by Brayton et al. (1972). The description of the complete package of solver routines and its applications to the r-process calculations, can be found in Blinnikov & Panov (1996). A similar full network is developed by Goriely & Arnould (1996).

Nuclear reaction rates were taken mainly from Thielemann et al. (1986), and mass relations from Hilf et al. (1976), though we also considered the dependence of r-process yields on various mass relations and nuclear reaction sets. Beta-decay rates were taken from Aleksankin et al. (1981). We evaluated the influence of different sets of beta-decay rates, either. The comparison with beta-decay rates of Staudt et al. (1990) shows, that for the majority of nuclei with even Z, the calculated values are rather close to each other. Nevertheless, for some isotopic chains with odd Z, the deviations may be rather large. However, all these deviations may affect significantly only the isotopic yields but not the elemental ones. Here we concentrate mainly on the efficiency of the neutrino-induced r-process under the astrophysical conditions expected for the helium shell while our discussion of influence of different nuclear data available is not so detailed; in particular, it concerns the beta-decay rates, beta-delayed neutron emission probabilities, and the rates

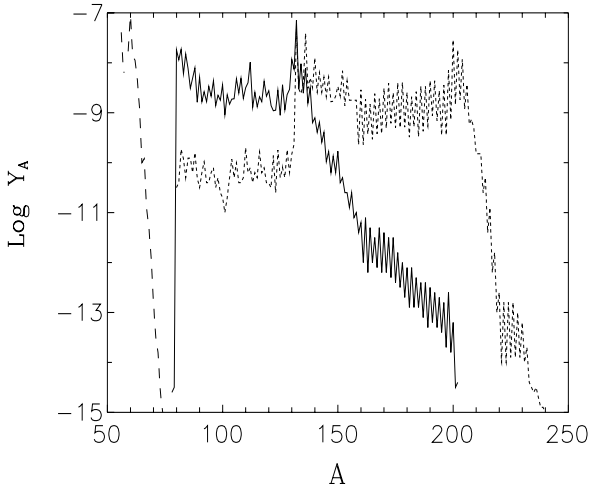

Fig. 6. The r-process abundances $Y_{\rm A} = \sum_Z Y(A,Z)$ as a function of atomic mass. Version I : $R = 5\times10^8$ cm, duration time $\tau = 10$ sec (solid line) and 35 sec (dotted line). Version II (dashed line): $R = 10^9$ cm, duration time $\tau = 100$ sec. Mass formulae are from Hilf et al. (1976).

of the electron neutrino nuclear capture. Results of the calculations are shown in Figs. 6 and 7 for Versions I and II and for various mass formulae. For Version I, independent of the mass formulae used, the nuclei from $A = 80$ through $A = 130$ and then up to $A = 200$ were synthesized by the 10-th and 35-th second, respectively. Under the conditions of Version II it is possible also to form some r-process nuclei but not far from the iron peak.

The differences in the shape of the abundance curves based on different data sets are not very high, except for the region of low A, where the initial nuclei burn out a little bit slower when the data of Hilf et al. (1976) and reactions rates of Thielemann (1986) are used instead of combining the data of Jänecke & Eynon (1976) with reactions rates of Panov (1995, 1997) (see Figs. 6 and 7).

In our network calculations, we have taken into account the emission of beta-delayed neutrons to study whether they are able to reduce the amplitude of the odd-even effect. The smoothing of abundances due to the emission of beta-delayed neutrons proved, however, to be small in our case, since the neutron flux is not very high and r-process nucleosynthesis occurs not far from the stable nuclei having small values of the beta-delayed neutron emission probabilities. This effect depends mostly upon the changes in r-process path after the break-down of nuclear statistical equilibrium and usage of the kinetic network of nucleosynthesis (Howard et al., 1993).

As it can be seen from Figs. 6 and 7, in the region of $A \gtrsim 150$ the odd-even effect is a little bit more pronounced – maybe because of the boundary effects such, for example, as a step-like shape of the stable nuclei boundary (Panov & Blinnikov, in preparation).

An additional smoothing of the odd-even effect could occur due to emission of the beta-delayed neutrons during subsequent beta-decays into stable isotopes. But under the astrophysical

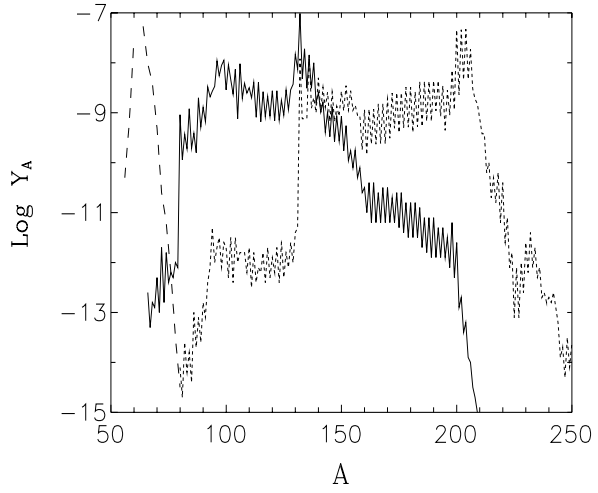

Fig. 7. Same as in Fig. 6, but Mass formulae are taken from Jänecke & Eynon (1976), and nuclear reaction rates from Panov (1995, 1997).

conditions discussed here, the r-process path lies not far from beta-stable nuclides and only a fraction of the nuclei formed in sufficient quantity have significant values of beta-delayed neutron emission probabilities. That is why in the present case the smoothing of the odd-even effect due to delayed neutrons happens to be small and cannot change significantly the calculated abundance curves.

6. Discussion and conclusions

In this work we began a systematic study of the conditions favorable for the neutrino-induced production of free neutrons in the amounts sufficient to form heavy elements through the r-process in stellar shells surrounding the collapsed core — a source of the intense neutrino flux. The problem in question is described by four main parameters: radius of the shell R (the neutrino flux scales as R^{-2}), density ρ, and temperature T in the shell, and chemical composition of the shell. The latter parameter splits in two important ones — the main constituent (helium, carbon, silicon etc.) and the admixture of the neutron poison species like ^{14}N and ^{56}Fe, the latter being both a raw material for the r-process and a neutron poison as well. We concentrate here on the possibility of the r-process in a helium shell consuming neutrons from the breakup of ^{4}He by neutrinos.

We explored the dependence of the neutron yield, $Y_{\rm n}$, on R varying within 4×10^8 – 4×10^9 cm (Fig. 4) for constant values of temperature, density, and metallicity: $T_9 = 0.2$, $\rho = 3\times10^3$ g cm^{-3}, and Z$= 0.01$Z$_\odot$. The calculations of the r-process with $Y_{\rm n}(t)$ given by the curves for $R = 5\times10^8$ and 10^9cm in Fig. 4 show that there exists a critical radius of the helium shell $R_{\rm cr} \approx 10^9$cm, above which the neutrino flux fails to stimulate the r-process efficiently.

The calculations of $Y_{\rm n}$ for different temperatures of the helium shell (Fig. 5) demonstrated a strong sensitivity of $Y_{\rm n}$ to temperature. It was also shown that in accurate calculations one has to take into account the heating of helium shell by neutrinos, especially if the density is large enough $\left(\rho \gtrsim 10^5 \text{g cm}^{-3}\right)$. For the initial temperature $T_9 \gtrsim 0.5$, $Y_{\rm n}$ begins to increase with temperature, first at the very onset of the neutrino flux and then progressively at longer times (compare curves $T_9 = 0.5$ and 0.8 in Fig. 5). If the initial temperature of the helium shell happens to be as large as $T_9 \approx 2$, one can expect a certain increase in the critical radius $R_{\rm cr}$. From one side, such temperatures prevent the neutrino-destroyed helium to be reassembled and thereby support $Y_{\rm n}$ at a higher level. From the other side, at such a high temperature, thermonuclear reactions (γ,p), (γ,n), (p,n), (α,n) become fast enough to contribute themselves to $Y_{\rm n}$ even when the neutrino flux is absent (Woosley et al., 1990).

It is worth noticing that the shock wave, passing across the helium shell in a few seconds after the collapse of stellar core, heats matter up to $T_9 = 2$–3 and reprocesses the products of the neutrino-induced nucleosynthesis. This effect deserves more detailed study. Here we would like only to mention an interesting chance (see also Domogatsky et al., 1978b) given by a possibility of collapses not leading to standard powerful supernova explosions. This chance can be high if, e.g., the neutron star formation rate is higher than the rate of collapsing supernova outbursts. Unfortunately, the uncertainties of observations do not permit to prove this to be true, yet they do not reject this chance, either. It is conceivable, that the rotation of a presupernova plays the major role during those almost silent collapses. So, a large mass of the material would be kept at the radius lower than $R_{\rm cr}$ by the angular momentum conservation. Later, as suggested by Bisnovatyi-Kogan (1970, 1980), the magnetic field, enhanced by the differential rotation, can eject the outer layers (already irradiated by the neutrino flux). It is interesting to note that the latest computations (Bisnovatyi-Kogan et al., 1995) fail to produce an explosion on the supernova energy scale. So, a powerful shock wave, able to dissociate the r-process nucleosynthesis yields, is not formed, but the mechanism seems to be able to eject (with relatively low velocity) an amount of r-elements sufficient for enrichment of the interstellar matter.

However, it is not yet clear quantitatively how important the possible changes both in the rates λ_β, $\lambda_{\nu e}$, and their ratios could be for the neutrino nucleosynthesis issues. These changes are connected with a possible dependence of λ_β and $\lambda_{\nu e}$ on temperature and density owing to, for example, the contribution of excited nuclear states and the Pauli principle for electrons.

The conditions chosen by us, in particular $R = 5\times10^8$ cm, appear to be privileged in a certain sense. Here the supernova neutrino pulse leads to a neutron yield already sufficient to support the r-process through helium breakup, but it is not yet adequate for the *direct* formation of heavy nuclei during the r-process due to an increase in the neutron excess by the electron neutrino absorption and the neutrino-induced evaporation of neutrons from heavy nuclei (Domogatsky & Nadyozhin, 1978). Fig. 8 shows the influence of the neutrino capture by heavy nuclei on the r-process. In order to single out this effect, the emission of beta-delayed neutrons was not included in these two runs. We see only an acceleration of the r-process but it is hard to find any additional smoothing of the odd-even effect.

When R decreases, the rate $\lambda_{\nu e}$ increases, and the growth of the element synthesis due to neutrino capture relative to the

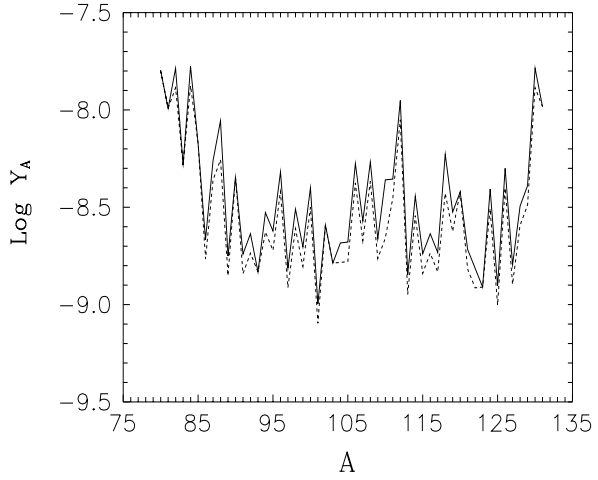

Fig. 8. The influence of the neutrino capture by heavy nuclei on the r-process for duration $\tau = 10$ sec (the capture is on — solid line, off — dashed line; $Y_{\rm n}(t)$ for Case 6).

beta-decays at the waiting points can lead finally to smoothing of the element yield curve. This issue, however, needs further investigation.

Recently, it was shown that the extremely metal poor stars are made of matter enriched with heavy elements synthesized in a well developed r-process (Cowan et al., 1996a, 1996b; Ryan et al., 1996; Sneden et al., 1996). In the near future, we are going to extend our calculations to metallicities as low as Z$= 0.001$Z$_\odot$ and even less to estimate the resulting increase in $R_{\rm cr}$.

In general, we conclude that it is very difficult to obtain the neutrino-induced r-process in a helium shell at radii $R > R_{\rm cr} \approx 10^9$cm, in a good agreement with Woosley et al. (1990). The current presupernova models have radii of the helium shell at least several times larger than $R_{\rm cr}$ specified above. Nevertheless, we continue to search for the physical conditions appropriate for the neutrino-driven r-process, not binding ourselves with the question of compatibility with the current presupernova models and having in mind probable modifications of the models involved, in particular, large scale convection, rotation, and magnetic fields.

Acknowledgements. Part of this work was done during the stay of D.K.N. in the Astronomical Institute University of Basel and kindly supported by Swiss National Science Foundation. It is a great pleasure for D.K.N. to acknowledge the support and to thank Prof. G.A. Tammann for heartfelt hospitality.

I.V.P. also gratefully acknowledges the hospitality of the MPA and Max Planck Gesellschaft for the opportunity to finish this work and fulfill numerical computations at MPI für Astrophysik. We are grateful to Prof. F.-K. Thielemann for providing us with his database of thermonuclear reaction rates and to S.E. Woosley and A.M. Bykov for stimulating discussions. The work was also supported by grants Nos. 96-02-17604 and 96-02-16352 of Russian Foundation of Fundamental Research (RFFI) and ISTC Project No 370-97.

Our special thanks to B.S. Meyer (the Referee) whose constructive critics prompted us to improve both the text and contents of the paper.

Appendix A: a selfconsistent solution for $Y_{\rm n}$

We use two nuclear kinetic codes. One deals with 101 reactions involving 24 light nuclides from ^{1}H and n through ^{18}F (Code L hereafter), listed in Tables 1 and 2. In addition, it takes into account the absorption of neutrons and protons by ^{56}Fe. Another code (Code H), designed for studying the r-process, connects more than 3000 heavier nuclides in a network of neutron-capture reactions and beta-decays. The two codes are physically connected through the exchange of neutrons (the proton-capture by Fe in Code L is virtually unimportant at rather low temperatures considered here). The r-process converts initial Fe into heavier nuclei which continue to absorb neutrons at a rate that changes as the r-process nucleosynthesis "wave" reaches successively heavier and heavier nuclei. Fig. 3 shows the results of various assumptions concerning the rate of the neutron absorption in the r-process, made in Code L, to supply Code H with the neutron abundance $Y_{\rm n}(t)$ that would permit to calculate the r-process without appealing to Code L any more. Case 6 was chosen as a compromise.

There are two ways to check the accuracy of such an approximation. The most straightforward way would be to unify the two networks in one code. This time-consuming work has been planned for the future. Another way is to iterate $Y_{\rm n}(t)$ function as described below.

First, one calculates the r-process using an approximate solution for time-dependent neutron density $Y^0_{\rm n}(t)$ from Code L instead of Eq.(18). The calculations provide the rate of the neutron density change, required by the r-process $\dot{Y}^0_{\rm n}(t)$ and given by the right-hand side of Eq.(18). Then, using this $\dot{Y}^0_{\rm n}$ one begins to run Code L with slightly modified differential equation for $Y_{\rm n}$:

$$dY_{\rm n}/dt \;=\; B \,+\, Y_{\rm n}\, f^0(t)\,, \qquad \text{(A1)}$$

where $f^0(t) \equiv \dot{Y}^0_{\rm n}(t)/Y^0_{\rm n}(t)$ and B denotes all the neutron absorbing and emitting reactions given in Tables 1 and 2 except for the reaction Fe(n,γ). In Case 6, the second term in the right-hand side of Eq.(A1) equals exactly to the unmodified right-hand side of Eq.(16) as described in Sect. 4. As a result of this Code L run one gets an iterated function $Y^1_{\rm n}(t)$. Entering Code H again, now with $Y^1_{\rm n}(t)$, one obtains $\dot{Y}^1_{\rm n}(t)$ that gives the second approximation $Y^2_{\rm n}(t)$ for $Y_{\rm n}(t)$ after running Code L and so on ...

Fig. A1 shows the results of such an iterative fairly fast-converging procedure. It takes 4–5 iterations to get the final selfconsistent solution shown in Fig. A1 with stars nonconnected by line. The thin line underlying the stars represents the last but one iteration that is almost indiscernible from the final solution.

From Fig. A1, one can conclude that Case 6 ensures a reasonable approximation for $Y_{\rm n}(t)$ as long as $t \lesssim 5$ s. However, for longer time ($t \gtrsim 10$ s), Case 6 overestimates $Y_{\rm n}(t)$ by an order of magnitude — the r-process consumes about 90% of neutrons provided by the neutrino breakup of ^{4}He. We remind that in Case 6 initial Fe proves to be totally burnt by $t \approx 1$ s. Therefore for longer times, Case 6 actually neglects the absorption of neutrons by the r-process. Using the selfconsistent

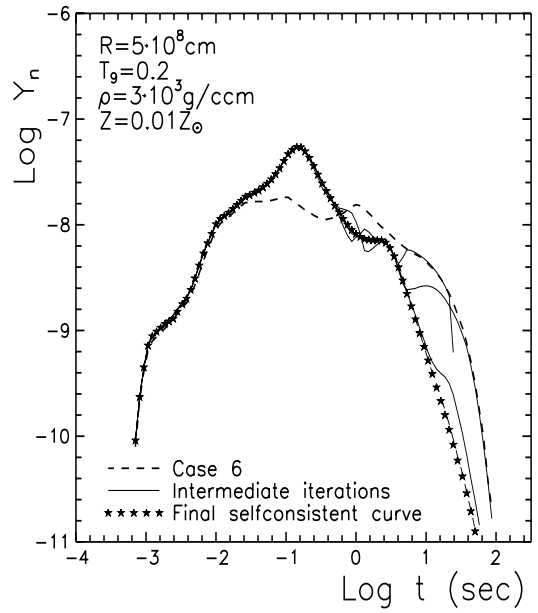

Fig. A1. The iterative procedure converting the initial approximate $Y_{\rm n}(t)$ for Case 6 (dashed line) into a final selfconsistent solution (stars).

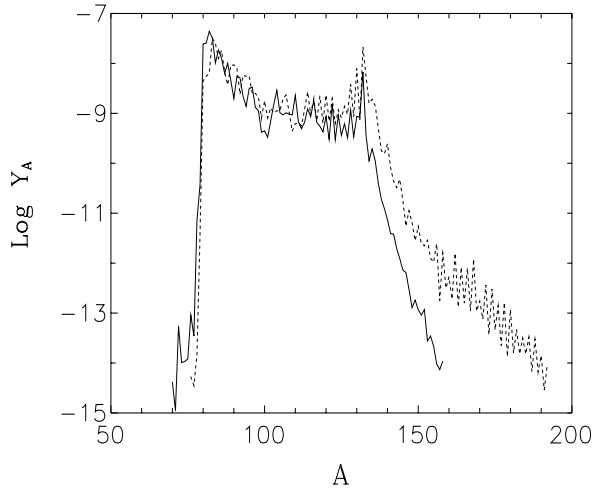

Fig. A2. Same as Version I in Fig. 6 but for selfconsistent $Y_{\rm n}(t)$ from Fig. A1.

solution for $Y_{\rm n}(t)$ (stars in Fig. A1) instead of that for Case 6 (dashed curve in Fig. A1), we have recalculated the r-process for times $t = 10$ and $35\,$s as shown in Fig. A2. Although the r-process yields changed at $t = 10\,$s but not so significantly as to alter our conclusions in the main text of the paper. At $t = 35\,$s, the changes are crucial — owing to a shortage in neutrons, the r-process gets virtually exhausted and fails to form the abundance peak at $A \approx 200$. To make the r-process as far as $A = 200$ and beyond under physical conditions discussed here ($T_9 = 0.2, R = 5\times10^8$ cm) one needs apply to lower metallicities ($\mathrm{Z} < 0.01\,\mathrm{Z}_\odot$). For the selfconsistent solution, the total number of neutrons consumed in the r-process per seed ^{56}Fe nucleus is equal to about 50.

References

Aleksankin V.G., Lyutostansky Yu.S., Panov I.V., 1981, Sov. J. of Nucl. Phys. 34, 1451.

Anders E. & Grevese N., 1989, Geochim. Cosmochim. Acta 53, 197.

Aufderheide M.B., Fushiki I., Woosley S.E., Hartmann D.H., 1994, ApJS 91, 389.

Bazan G. & Arnett D., 1994, ApJ Lett. 433, L41.

Bisnovatyi-Kogan G.S., 1970, AZh 47, 813.

Bisnovatyi-Kogan G.S., 1980, Ann. NY Acad. Sci. 336, 389.

Bisnovatyi-Kogan G.S., Moiseenko S.G., Ardelyan N.V., 1995, Preprint SRI No 1917, Moscow; Astrophys. Space Sci. (in press).

Blinnikov S.I. & Panov I.V., 1996, Pis'ma AZh — Astronomy Letters 22, 39.

Blinnikov S.I., Dunina-Barkovskaya N.G., Nadyozhin D.K., 1996, ApJS, 106, 171. Published earlier as Preprint No 78 (1994) Astr. Inst. University of Basel and Preprint No 943 (1996) Max-Planck-Institut für Astrophysik (improved version).

Brayton R.K., Gustavson F.G., Hachtel G.D., 1972, Proc. of Institute of Electrical and Electronics Engineers. New York. 60, 98.

Caughlan G. & Fowler W., 1988, Atomic Data Nucl. Data Tables 40, 283.

Clayton D.D., 1989, ApJ 340, 613.

Cowan J.J., Truran J.W., Burris D.L., 1996a, ApJ Lett. 460, L115.

Cowan J.J., Sneden C., Truran J.W. et al., 1996b, in Proceedings of the Fourth Int. Conf. *Nuclei in the Cosmos*, Notre Dame, June 20–27. Eds. Görres J., Mathews G., Wiescher M., Shore S. Amsterdam: ELSEVIER. Nuclear Phys. A621, 41c.

Domogatsky G.V. & Nadyozhin D.K., 1977, MNRAS 178, 33p.

Domogatsky G.V. & Nadyozhin D.K., 1978, AZh – Sov. Astron. 22, 297.

Domogatsky G.V. & Nadyozhin D.K., 1980, Ap. Sp. Sci. 70, 33.

Domogatsky G.V. & Imshennik Svetlana V., 1982, Pis'ma AZh — Sov. Astron. Lett. 8, 190.

Domogatsky G.V., Eramzhyan R.A., Nadyozhin D.K., 1978a, in Neutrino'77, Proc. Int. Conf. Neutrino Phys. and Astrophys. Eds. Markov M.A. et al., p. 115, Nauka, Moscow.

Domogatsky G.V., Eramzhyan R.A., Nadyozhin D.K., 1978b, Ap. Sp. Sci. 58, 273.

Epstein R.I., Colgate S.A., Haxton W.C., 1988, Phys. Rev. Lett. 61, 2038.

Fuller G.M. & Meyer B.S., 1995, ApJ 453, 792.

Gear C.W., 1971, Numerical Initial Value Problems in Ordinary Differential Equations. Englewood Cliffs, New Jersey: Prentice-Hall.

Goriely S. & Arnould M., 1996, A&A 312, 327.

Hilf E.R., Groote H.V., Takahashi K., 1976, CERN-report. CERN-76-13, p. 142.

Hoffman R.D., Woosley S.E., Qian Y.-Z., 1997, ApJ 482, 951.

Howard W.M., Goriely S., Rayet M., Arnould M., 1993, ApJ 417, 713.

Jänecke J. & Eynon B.P. Atomic Data Nucl. Data Tables, 1976, 17, 467.

McLaughlin G.C. & Fuller G.M., 1995, ApJ 455, 202.

Meyer B.S., Mathews G.J., Howard W.M., Woosley S.E., Hoffman R.D., 1992, ApJ 399, 656.

Nadyozhin D.K., 1978, Ap. Sp. Sci. 53, 131.

Nadyozhin D.K., 1991, in Proceedings of the 6th Workshop on Nuclear Astrophysics. Eds. W. Hillebrandt & E. Müller, p. 76.

Nadyozhin D.K. & Panov I.V., 1993, in Proceedings of the 3d International Symposium on Weak and Electromagnetic Interactions in Nuclei (WEIN-92). Ed. Tc. Vylov. World Scientific Publishing Co., Utopia Press, Singapore, p. 479.

Nadyozhin D.K. & Panov I.V., 1997, in Proceedings of the Fourth Int. Conf. *Nuclei in the Cosmos*, Notre Dame, June 20–27, 1996. Eds. Görres J., Mathews G., Wiescher M., Shore S. Amsterdam: ELSEVIER. Nuclear Phys. A621, 359c.

Nadyozhin D.K., Panov I.V., Blinnikov S.I., 1996, in Proceedings of the 8th Workshop on Nuclear Astrophysics. Eds. W. Hillebrandt & E. Müller, 1996, MPA/P9, p. 63.

Okun L.B., 1982 Leptons and quarks. Amsterdam: North Holland, ch. 16.

Panov I.V., 1994, Pis'ma AZh — Astronomy Letters. 20, 616.

Panov I.V., 1995, in Proceedings of Int. Conference on Nuclear Spectroscopy and Structure of Atomic Nuclei. St. Petersburg, Nauka. Ed. Gridnev, p. 358.

Panov I.V., 1997, Izvestija Rossijskoj Akademii Nauk, Serija Fizicheskaja 61, 210.

Qian Y.-Z. & Woosley S.E., 1996, ApJ 471, 391.

Ryan S.G., Norris J.E., Beers T.C., 1996, ApJ 471, 254.

Sneden C., McWilliam A., Preston G.W. et al., 1996, ApJ 467, 819.

Staudt A., Bender E., Muto K., Klapdor-Kleingrothaus H.V., 1990, Atomic Data Nucl. Data Tables 44, 79.

Takahashi K., Witti J., Janka H.-Th., 1994, A&A 286, 857.

Thielemann F.-K., Arnould M., Truran J.W., 1986, in Proceedings of the 2-nd Workshop "Advances in Nuclear Astrophysics". Eds. E. Vangioni-Flam et al. Edition Frontiers, p. 525.

Tuli J.K., 1990, Nuclear Wallet Cards. Upton, NY: National Nuclear Data Center.

Vogel P. & Engel J., 1989, Phys. Rev. D 39, 3378.

Wrean P.R., Brune C.R., Kavanagh R.W., 1994, Phys. Rev. C 49, 1205.

Weaver T.A. & Woosley S.E., 1993, Phys. Rep. 227, 65.

Woosley S.E. & Weaver T.A., 1995, ApJS 101, 181.

Woosley S.E., Hartmann D.H., Hoffman R.D., Haxton W.C., 1990, ApJ 356, 272.